

Pre-reforming of *n*-tetradecane over Ni/MgO–Al₂O₃ catalyst: effect of added potassium on the coke resistance

Sung-hun Lee^{1,2} · Kee Young Koo¹ · Un Ho Jung¹ · Yong-Gun Shul² · Wang Lai Yoon¹

Received: 6 May 2015 / Accepted: 12 September 2015 / Published online: 25 September 2015
© Springer Science+Business Media Dordrecht 2015

Abstract We investigated the pre-reforming of *n*-tetradecane (C₁₄H₃₀) over the K-promoted 50 wt% Ni/MgO–Al₂O₃ catalyst and also analysed the coke resistance. The 50 wt% Ni/MgO–Al₂O₃ catalysts were prepared by the deposition–precipitation method and 1–5 wt% of potassium was added to the catalyst using the impregnation method. The catalysts were characterized by ICP, XRD, H₂-chemisorption, H₂-TPR, and BET. The pre-reforming of *n*-tetradecane was performed under the reaction conditions of S/C = 4.0, GHSV = 3000 h⁻¹, and 400–450 °C. The Ni crystallite size increased, whereas the Ni dispersion and surface area of catalysts decreased with increasing amounts of K. The 50 wt% Ni/MgO–Al₂O₃ showed large amounts of coke deposition compared to the K-promoted catalysts. It was found that the K addition over 50 wt% Ni/MgO–Al₂O₃ catalyst was beneficial for coke removal by promoting the coke gasification. A 1 wt%K/50 wt% Ni/MgO–Al₂O₃ catalyst showed stable activity during pre-reforming at S/C = 4.0, GHSV = 3000 h⁻¹, and 400 °C. Furthermore, it had the lowest amount of surface coke, as observed by SEM, TEM, and TG analysis.

Keywords *n*-Tetradecane · Pre-reforming · Ni catalyst · Coke resistance · K/Ni/MgO–Al₂O₃

✉ Yong-Gun Shul
shulyg@yonsei.ac.kr

✉ Wang Lai Yoon
wlyoon@kier.re.kr

¹ Hydrogen Laboratory, Korea Institute of Energy Research (KIER), 152, Gajeong-ro, Yuseong-gu, Daejeon 305-343, Republic of Korea

² Department of Chemical and Biomolecular Engineering, Yonsei University, Yonsei-ro 50, Seodaemun-gu, Seoul 120-749, Republic of Korea

Introduction

Diesel comprises large hydrocarbon molecules C_8 – C_{21} , consisting of paraffin-based saturated hydrocarbons (75 %) and some aromatic compounds (25 %), and a small volume of sulfur [1, 2]. However, prior to using diesel in practical applications such as fuel cell systems, it needs to be subjected to a pre-reforming process. Pre-reforming process serves the following purposes: (1) all higher hydrocarbons are converted completely into C_1 compounds such as CH_4 , CO, and CO_2 , and hydrogen, (2) the traces of sulfur are adsorbed on the pre-reforming Ni catalyst, thereby minimizing sulfur poisoning and catalyst deactivation in downstream processes, (3) hot banding of the primary reformer can be avoided, and (4) the product gas can be heated up to 600–700 °C or higher without the risk of thermal cracking [1–9]. However, during the direct reforming of diesel, the catalyst can become poisoned by the presence of sulfur, and by coke formation at temperatures above 600 °C. This can hamper stable operation of the reforming process. For this reason, pre-reforming with a Ni catalyst at lower temperatures (350–550 °C) is necessary [1–6].

Ni-based catalysts are widely used commercially for pre-reforming due to their outstanding performance and cost-effectiveness. However, they become easily deactivated by coke formation [5, 10, 11]. Deposited coke is categorized into two types. The gum type is observed under 500 °C, and it causes catalyst deactivation by covering active sites of the catalyst due to the polymerization of CH_x . The whisker type is formed when higher hydrocarbon compounds are broken into olefin forms as a result of thermal decomposition above 450 °C [5–7, 12, 13].

Diesel pre-reforming is normally conducted within the temperature range at 350–550 °C, where both types of carbon deposition can easily cause deactivation of catalysts. Therefore, pre-reforming catalysts with greater coking resistance are desirable. To this end, the following three methods have been considered. The first involves suppressing direct cracking by controlling catalyst acidity through the addition of alkali metals, eliminating coke formation by gasification [12–16]. The second method involves adding materials that are capable of storing and releasing oxygen, such as Ce, Zr, and Co, which remove deposited carbon in the form of CO_x [17–20]. The third method includes the addition of precious metals such as Pt, Rh, and Ru that promote the conversion of carbon to CH_x due to H_2 spillover [21, 22].

In particular, many studies suggest that the addition of alkali metals is effective in improving catalyst activation and stability through the suppression of carbon deposition. For example, Frusteri et al. [15] reported that the addition of K to Ni/MgO catalysts in the carbon dioxide reforming of methane (CRM) changes the electronic state of Ni, thereby improving the resistance to coking and sintering. They also suggested that the addition of an alkali metal induces an electron enrichment state in the active phase (Ni metal), suppressing the Boudouard reaction and hydrocarbon decomposition, and decreasing coke formation on the Ni catalysts [23]. Hou et al. [24] reported that small amounts of Ca added to the Ni catalyst used in the CRM increases Ni dispersion, strengthens the interaction between Ni and Al_2O_3 , and enhances the activity and stability of the catalysts by suppressing sintering. However, a mole ratio of at least $Ca/Ni = 0.2$ or higher was reported to

increase CH₄ decomposition, thereby accelerating carbon deposition and deactivating catalysts. Impregnation of K in Ni/Al₂O₃ catalysts for acetic acid reforming not only suppresses CH₄ generation, but also increases catalyst stability through gasification of deposited coke (Hu et al.) [14]. According to research conducted by Juan–Juan [25], the addition of K helped improve the reduction of Ni by hydrogen in the CRM reaction, because K affects the interaction between the support and NiO. They also discuss how K neutralizes the active sites.

Despite these studies, to the best of our knowledge, the target reactants in the preceding studies are mostly limited to the light hydrocarbon series. This study investigated how the addition of K to a 50 wt%Ni/MgO–Al₂O₃ catalyst affected activity and carbon deposition during pre-reforming of *n*-tetradecane as an analogue for diesel feedstock.

Experimental

Catalyst preparation

The 50 wt%Ni/MgO–Al₂O₃ catalysts were prepared by a deposition–precipitation (DP) method [26]. This is because the impregnation method affords highly dispersed NiO nanoparticles for low contents of Ni (~10 wt%), but does not work very well for higher Ni contents (50 wt%). Thus, in the case of high loading amounts of Ni, it is possible to generate a highly dispersed Ni catalyst by the DP method. MgO–Al₂O₃ (MgO = 30 wt%, SASOL, BET S.A. = 204 m²/g), Ni(NO₃)₂·6H₂O (97 %, JUNSEI), KNO₃ (Extra pure, JUNSEI) were used as precursors of the prepared catalysts. The 10 % KOH solution (SIGMA-ALDRICH) was used as precipitation agent. The suspension of MgO–Al₂O₃ support was stirred with a mechanical hot plate stirrer in the distilled water at 80 °C. Ni(NO₃)₂·6H₂O solution and KOH solution were dropped in the support solution for 2 h. The pH of the solution was fixed at 11.5 and it was agitated for 24 h. The precipitate was washed out by the distilled water five times to remove residual salt. After the drying process in the air, it was calcined in air at 500 °C for 6 h. The 1, 3, 5 wt% of potassium were loaded on the calcined samples by the impregnation method and they were calcined in air at 500 °C for 6 h. Prepared catalysts were named 0K/50Ni, 1K/50Ni, 3K/50Ni, and 5K/50Ni, respectively.

Characterization

The content of metal in prepared catalysts was determined by inductively coupled plasma (ICP) in a OPTIMA Spectrometer 7300 DV (Perkin-Elmer). The composition and crystal structure of prepared catalysts were analyzed by X-ray diffraction (XRD, D/Max-2500pc, Rigaku) using Cu K_α radiation at a scanning speed of 2°/min and step width of 0.02° from 10° to 90° (2θ). The NiO crystallite size was estimated using the Scherrer equation. Temperature programmed reduction (TPR) analysis

was carried out to identify the reduction temperature and reducibility of the catalysts through BEL CAT B (BEL Japan Inc.). A 0.1 g of sample was loaded into a U-shape quartz reactor, and then pretreatment was carried out at 30 °C for 30 min under Ar gas. Then, it was heated by an electrical furnace at heating rate of 10 °C/min from 40 to 900 °C under 10 % H₂/Ar gas. The BET and BJH of catalysts were measured by Belsorp-max (BEL Japan Inc.) through the N₂ adsorption at -196 °C after the samples of 0.2 g were pretreated at 300 °C for 3 h under vacuum. H₂-chemisorption (BEL-METAL-3, BEL JAPAN INC.) was performed to observe metal dispersion, and metallic surface area. The sample of 50 mg was reduced in H₂ flow at 600 °C for 1 h. The sample was purged at 600 °C for 1 h in He flow and cooled to 50 °C. A H₂ pulse (20 % H₂/Ar) was injected into the catalyst. The adsorbed H₂ amount was obtained by assuming the adsorption stoichiometry of one hydrogen atom per nickel atom on the surface ($H/Ni_{\text{surface}} = 1$). The morphology of coke formation and size of Ni particle were observed through SEM (S-4700, HITACHI), and TEM (Tecnai F20, Philips). The coke amount was quantitatively determined by a thermogravimetry analyzer (TGA, Netzsch TG209F3). The sample of 50–70 mg was heated to 200 °C under N₂ condition for the elimination of H₂O. Then, the sample was heated from 30 to 800 °C with a heating rate of 5 °C/min in the air. The electron state of used catalysts was measured with an X-ray photoelectron spectroscope (XPS, MultiLab 2000, Thermo) and the binding energy (BD) was calibrated by using the C 1s peak at 284.6 eV as a reference.

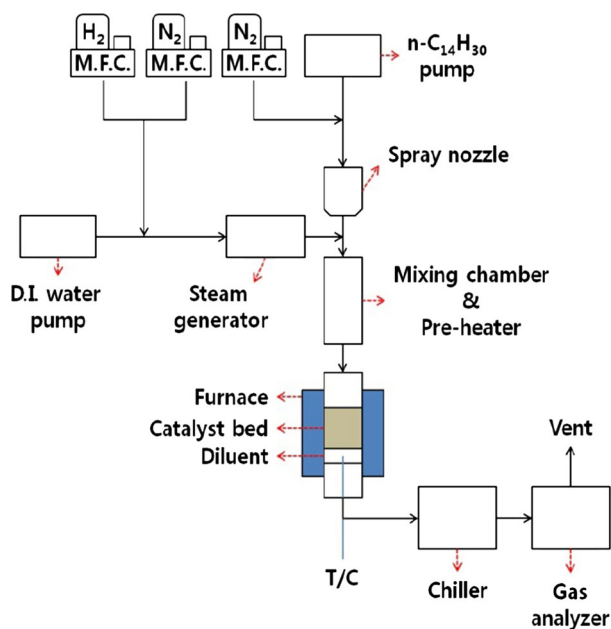


Fig. 1 Schematic diagram of the experimental apparatus for $n\text{-C}_{14}\text{H}_{30}$ pre-reforming reaction

Catalytic activity test

A catalytic activity test was performed at a reaction temperature of 400–450 °C, S/C ratio = 4.0, and gas hourly space velocity (GHSV) = 3000 h⁻¹. *n*-tetradecane (*n*-C₁₄H₃₀, Aldrich) was used as a surrogate compound of diesel based on our previous report [26]. A schematic diagram of the experimental apparatus for *n*-C₁₄H₃₀ pre-reforming reaction is shown in Fig. 1. The prepared catalyst and diluent were sorted into 60–100 mesh and mixed evenly. The mixture was charged in a fixed-bed 1/2" quartz reactor. A thermocouple was inserted inside the center of the diluent to fix the temperature at 400 and 450 °C. The catalyst was reduced at 600 °C for 4 h under 10 % H₂/N₂ before the reaction test. Steam was generated by a steam generator and *n*-tetradecane was atomized by a spray nozzle (UNP-60L, Sysonic & Green System Co. Ltd.). Next, generated steam was mixed with *n*-tetradecane and passed the mixing section. Uniformly mixed feedstock was heated up to 200 °C and supplied to the reactor. Trunfio et al. [27] reported that co-feeding of H₂ improves the stable operation of the catalyst. Therefore, 0.2 ml-H₂/mg-hydrocarbon was supplied [28]. The effluent was passed through a trap to condensate residual water, and the composition of gases was analyzed by on-line Micro-GC from Agilent 3000. The thermodynamic equilibrium value was calculated with HSC chemistry[®] 7.1 software on the basis of Gibbs energy minimization.

Results and discussion

Catalytic characterization

The prepared catalysts had K contents of 1.1, 2.8, and 4.8 wt%, as determined by ICP analysis (Table 1). Figure 2 shows the XRD peaks of the catalysts prepared with different contents of K as a promoter. The NiO peaks are observed at

Table 1 Characteristics of the K promoted 50 wt%Ni/MgO–Al₂O₃ catalysts

Sample	K content ^a (wt%)	Crystallite size (nm)		Metal dispersion ^d (%)	Metal surface area ^d (m ² /g)	Reduction degree ^e (%)	Surface area ^f (m ² /g)
		NiO ^b (fresh)	Ni ^c (reduced)				
0K/50Ni	0.0	4.4	4.9	8.5	56.9	26	188
1K/50Ni	1.1	5.0	6.0	7.4	49.3	28	178
3K/50Ni	2.8	4.9	8.4	7.2	48.1	30	159
5K/50Ni	4.8	5.1	12.2	5.5	36.3	42	126

^a Determined by inductively coupled plasma (ICP)

^b The values were calculated by Scherrer's equation $2\theta = 63.2^\circ$

^c The values were calculated by Scherrer's equation $2\theta = 51.6^\circ$

^d Estimated from H₂-chemisorption at 50 °C

^e Calculated from reduction of the catalyst at 600 °C for 1 h

^f Estimated from N₂ adsorption at -196 °C

$2\theta = 37.4^\circ$, 43.5° , 63.2° , 75.8° , and 79.9° . However, peaks for the MgO–Al₂O₃ support and added K₂O were not observed. The MgO–Al₂O₃ mixed oxide support exists as unstable MgO and Al₂O₃ before calcination, but changes into the form MgAl₂O₄ when the calcination temperature reaches 600 °C [26]. Therefore, only NiO peaks were observed in the prepared catalysts because the calcination temperature of 500 °C inhibited the crystalline growth of MgAl₂O₄. This result is in good agreement with previous research by Koo et al. [26]. The impregnated K is easily incorporated in NiO, so it is not likely to be observed through XRD analysis. [29] Table 1 shows the NiO crystallite sizes calculated using Scherrer's equation at $2\theta = 63.2^\circ$. Crystallite sizes were in the range of 4.4–5.1 nm, meaning that the NiO was highly dispersed within the catalyst and that the loading amounts of potassium did not affect the NiO crystallite size.

Figure 3 provides the results of XRD analysis of the reduced catalysts. Peaks for both Ni and unreduced NiO were found, which will be discussed later with the H₂-TPR results. Table 1 provides the Ni particle sizes measured at $2\theta = 51.6^\circ$. After reduction, particles of Ni grew to 4.9–12.2 nm as the K content increased from 0 to 5 wt%. This observation is similar to that of Nobuhiro Iwasa [30], in which the Ni particle size grew from 14 to 124 nm as a result of increasing K content from 0 to 10 wt%, when Ni-containing smectite materials with potassium was reduced at 700 °C. These results demonstrate that impregnation of K led to agglomeration of Ni particles during the reduction of NiO to Ni, and the increase in K content was observed to be correlated with an increased Ni particle size.

Next, we conducted H₂-chemisorption analysis in order to measure the degree of dispersion and surface area of Ni. We found that the degree of dispersion and surface area of Ni reduced as the content of added K increased. This result coincides with the changes in Ni sizes observed in XRD analysis.

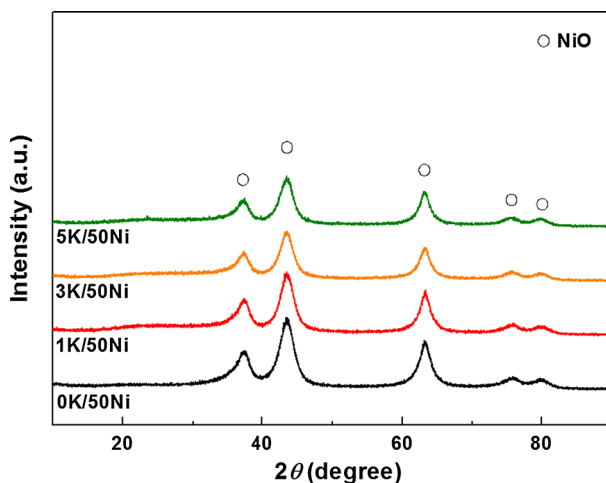


Fig. 2 XRD patterns of the K-promoted 50 wt%Ni/MgO–Al₂O₃ catalysts

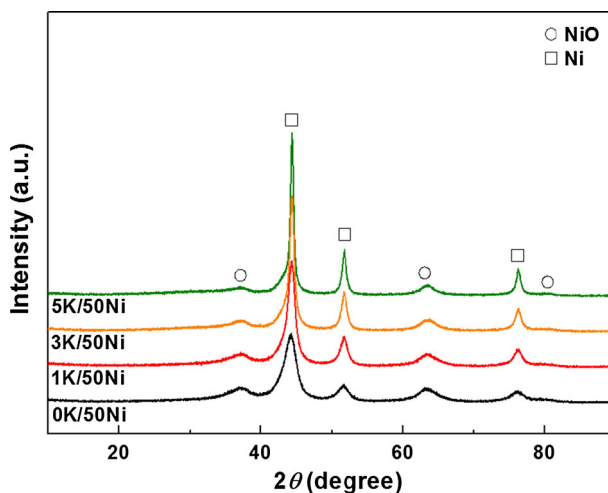


Fig. 3 XRD patterns of the K-promoted 50 wt% Ni/MgO–Al₂O₃ catalysts after reduction at 600 °C for 4 h

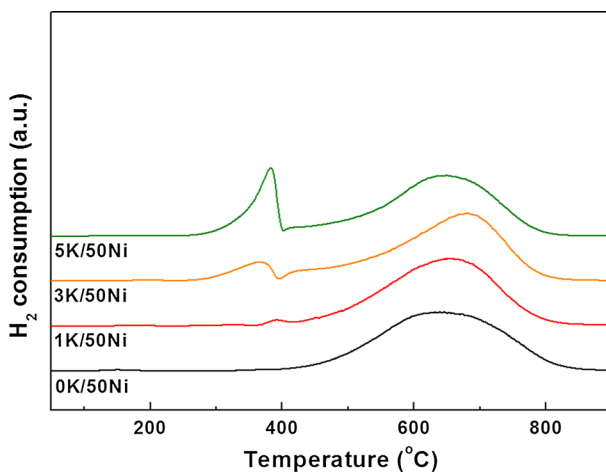


Fig. 4 TPR profiles of the K-promoted 50 wt% Ni/MgO–Al₂O₃ catalysts

The TPR results in Fig. 4 show that peaks corresponding to highly dispersed Ni particles on the support are observed for all catalysts at a temperature of 600 °C or higher. The peak intensity of free NiO observed at 400 °C or lower increased as K content increased, resulting from the fact that the addition of K affects the interaction of the support and NiO [14, 25]. In general, free NiO can be formed by a weak interaction between the support and NiO. This in turn can inhibit stable catalyst activity. Table 1 shows the degree of catalyst reduction calculated from the reduced area at or below 600 °C, the actual reduction temperature. As K content

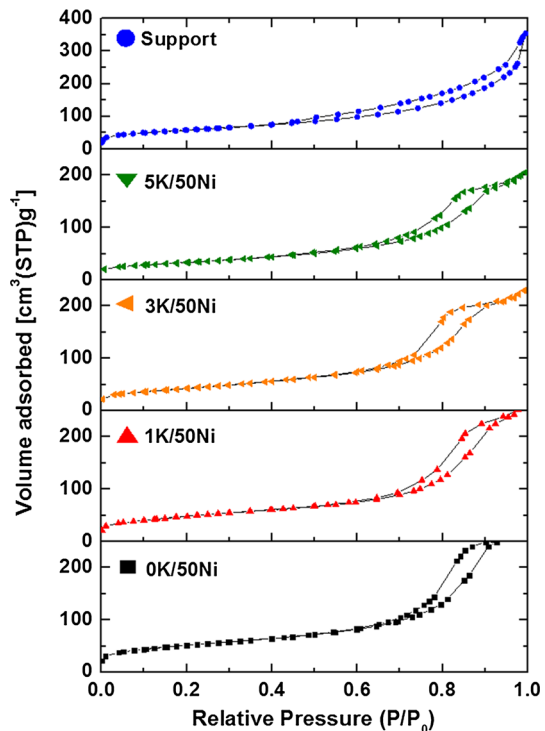
increased, the amount of reduced NiO also increased because the reduced area was affected by free NiO, as mentioned earlier (Fig. 4). For catalysts with free NiO, the Ni crystallite size grew larger during reduction; which is expected to decrease catalytic activity. Since NiO is mostly reduced at temperatures in excess of 600 °C, NiO peaks were observed in the XRD pattern.

Catalyst surface areas, measured by BET, decreased from 188 to 126 m²/g as a result of increasing K. The N₂ adsorption–desorption isotherm of the support and prepared catalysts (Fig. 5), shows type IV hysteresis, corresponding to a mesoporous catalyst structure. The hysteresis loop results from a capillary phenomenon that arises from the existing pores in the catalysts. Formation of the hysteresis loop is affected by the pore size and volume [31, 32]. Figure 6 shows the pore size distribution of the support and prepared catalysts, measured by the BJH method. In the case of support, mesopores and macropores were developed. However, the pore size distribution of prepared catalyst showed pores of 12.2 nm to be the most developed.

Catalytic test in pre-reforming

Activity tests were conducted to examine the performance and stability of the catalysts. Figure 7 and Table 2 summarize the results for pre-reforming of C₁₄H₃₀ compounds at 450 °C. The 0K/50Ni, 1K/50Ni, and 3K/50Ni catalysts afforded CH₄

Fig. 5 N₂ adsorption–desorption isotherms of the K-promoted 50 wt% Ni/MgO–Al₂O₃ catalysts



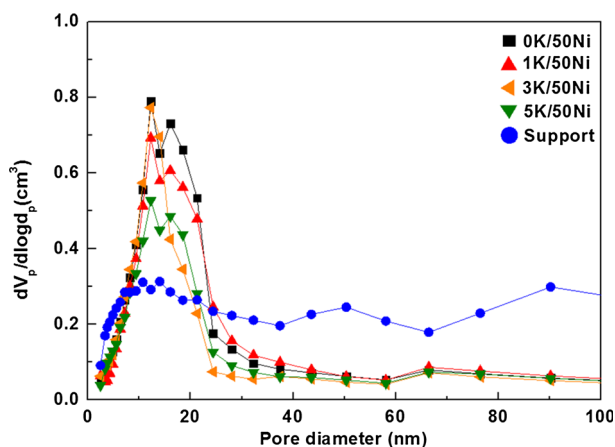


Fig. 6 The pore size distribution of the K-promoted 50 wt% Ni/MgO–Al₂O₃ catalysts

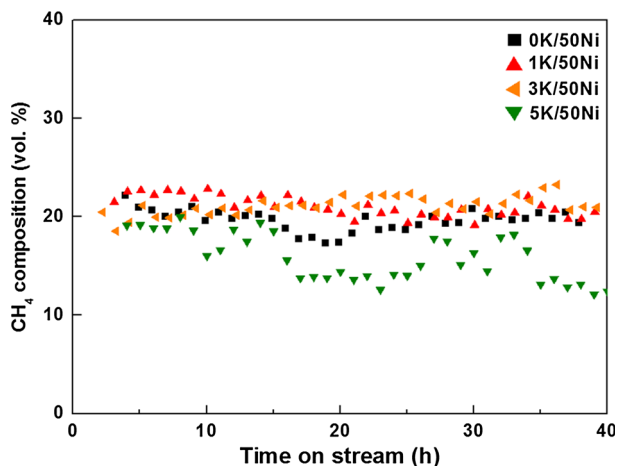


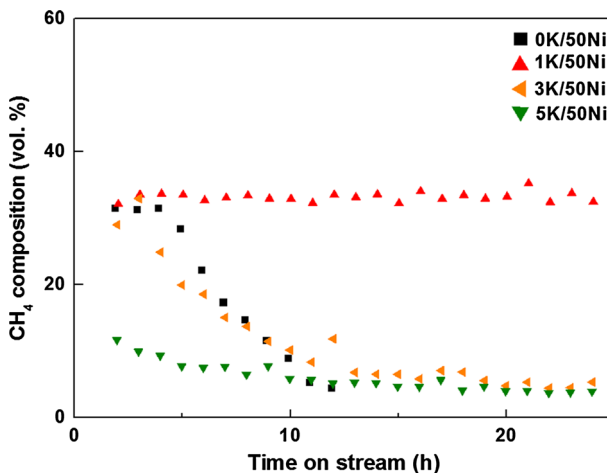
Fig. 7 CH₄ composition of the K-promoted 50 wt% Ni/MgO–Al₂O₃ catalysts at 450 °C in pre-reforming (GHSV = 3000 h⁻¹, S/C = 4.0)

exit concentrations of 19.7–21.1 %, close to the equilibrium value of 20.7 %. However, 5K/50Ni catalyst gave a CH₄ exit concentration 5 % lower and CO concentration 1 % higher. This result agrees with that observed by Xun Hu [14], in that the impregnation of a larger amount of K suppresses methanation.

For a clearer comparison of the difference in catalytic activity, an experiment was carried at a lower operating temperature of 400 °C. Figure 8 demonstrate the results of pre-reforming of C₁₄H₃₀ compounds at 400 °C. Compared to the results obtained at 450 °C, the difference in CH₄ composition with added K content was found to be clearer at 400 °C. This is because, as the reaction temperature decreases, the reaction rate is decreased. Additionally, the catalytic activity depends on the

Table 2 Gas product composition in *n*-tetradecane pre-reforming on stream (reaction condition: $T = 450\text{ }^{\circ}\text{C}$, $\text{GHSV} = 3000\text{ h}^{-1}$, $\text{S/C} = 4.0$, $\text{TOS} = 40\text{ h}$)

Sample	CH_4	CO	CO_2	H_2
0K/50Ni	19.7	1.1	21.6	57.5
1K/50Ni	21.1	1.1	21.5	56.3
3K/50Ni	21.0	1.2	21.5	56.3
5K/50Ni	15.9	2.7	22.0	60.3
Equilibrium composition	20.7	1.2	23.3	54.8

**Fig. 8** CH_4 composition of the K-promoted 50 wt% Ni/MgO– Al_2O_3 catalysts at $400\text{ }^{\circ}\text{C}$ in pre-reforming ($\text{GHSV} = 3000\text{ h}^{-1}$, $\text{S/C} = 4.0$)

surface area of the active site. Therefore, the catalyst with smaller surface area and lower Ni dispersion shows lower activity. Interestingly, however, 0K/50Ni catalyst shows lower activity than the 1K/50Ni catalyst despite having high Ni dispersion and a high surface area. We believe this could be owing to deactivation of the 0K/50Ni catalyst by rapid poisoning of Ni active sites by the gum-type coke formed at $400\text{ }^{\circ}\text{C}$ [26]. From these results, we made two very interesting conclusions: (1) there is a minimum amount of K that needs to be added to stabilize the catalyst against coke poisoning, and (2) the initial activity decreased with increasing K content. This observed reduction in activity is consistent with the XRD and H_2 -chemisorption results, showing increased Ni particle sizes after reduction, and the decrease in surface area of metals. This is in agreement with the study conducted by Juan–Juan [25] who found that added K surrounded active Ni site located in step sites during reduction and reaction, decreasing available active sites. For the 1K/50Ni catalyst, the CH_4 exit concentration was 31 %, close to the equilibrium value of 32 %, and stable performance was observed over time changes.

Coke study

Coke deposition on used catalysts was analysed by SEM, TEM, TG analysis, and XPS after 40 h pre-reforming of *n*-tetradecane at $T = 450\text{ }^{\circ}\text{C}$, $\text{GHSV} = 3000\text{ h}^{-1}$, and $\text{S/C} = 4.0$. Also, the SEM and TEM analyses on the fresh samples were conducted to compare with the used samples clearly. It was noted that potassium oxide with rod-like shape was formed as the amount of K increased (Fig. 9). For the 0K/50Ni catalyst, SEM and TEM analyses showed that a large amount of whisker-type coke was formed on the surface of used catalyst (Figs. 9, 10). Ni particles were found to be detached from the support when the amount of deposited coking increased (Fig. 10). In comparison, the amount of whisker-type coke formed on the surface of the K-impregnated catalyst decreased significantly, because K accelerated the gasification of coke on the catalyst surface. This agrees with the preceding studies using lighter feedstocks that found that adding K reduced coke deposition through gasification [11, 15, 33, 34].

Table 3 provides the results of the TG analysis of the used catalysts after 40 h of pre-reforming at $450\text{ }^{\circ}\text{C}$. The amount of coke deposited on the 0K/50Ni catalyst was $0.0797\text{ gC/g}_{\text{cat}}$, which suggests that a considerable amount of coke was deposited compared to the catalyst with added K ($0.0200\text{--}0.0373\text{ gC/g}_{\text{cat}}$). Catalysts with added K indicated that the addition of an alkali metal such as K induced steam adsorption, thereby accelerating the gasification of coke deposited on the catalyst surface and suppressing coke deposition. However, among the K-promoted catalysts, as the amount of K increases, the amount of coke deposition increases. It was related with the change of Ni particle size, which had a significant effect on the coke deposition. According to a previous report, Koo et al. [35] explained that large Ni particles with a weak metal to support interaction were susceptible to coke formation. Thus, excess amounts of potassium led to the growth of Ni particles, which results in the coke deposition on the catalyst surface.

Table 4 lists the crystallite sizes of the reduced and used samples, measured using XRD analysis. For the 0K/50Ni catalyst, the size of NiO and Ni particles before and after reduction was similar (4.4 and 4.9 nm, respectively). However, we observed a distinct relation between Ni particle sizes after reduction and the amount of added K, which suggests that the addition of K contributes to growing Ni particles over the process of reduction. Interestingly, XRD results of the used catalyst are fairly similar to those of the reduced sample, indicating that the Ni particles grow mainly during the reduction process. The specific surface area and pore characteristics of the used catalysts were measured using BET and BJH after 40 h of pre-reforming at $450\text{ }^{\circ}\text{C}$. The specific surface area of the fresh sample was observed to decrease with increasing K content, and the specific surface area decreased over the course of catalyst reduction. After reduction, the pore diameters of the prepared catalysts (except for the 5K/50Ni catalyst) were similar, around 16.1 nm, which suggests that the addition of K (5 wt% or more) results in decreased specific surface area due to pore plugging [14, 30]. Also, we confirmed the differences of the binding energy of Ni 2p through the XPS analysis on the used samples (Fig. 11). As the amount of the potassium increases, the binding energy of

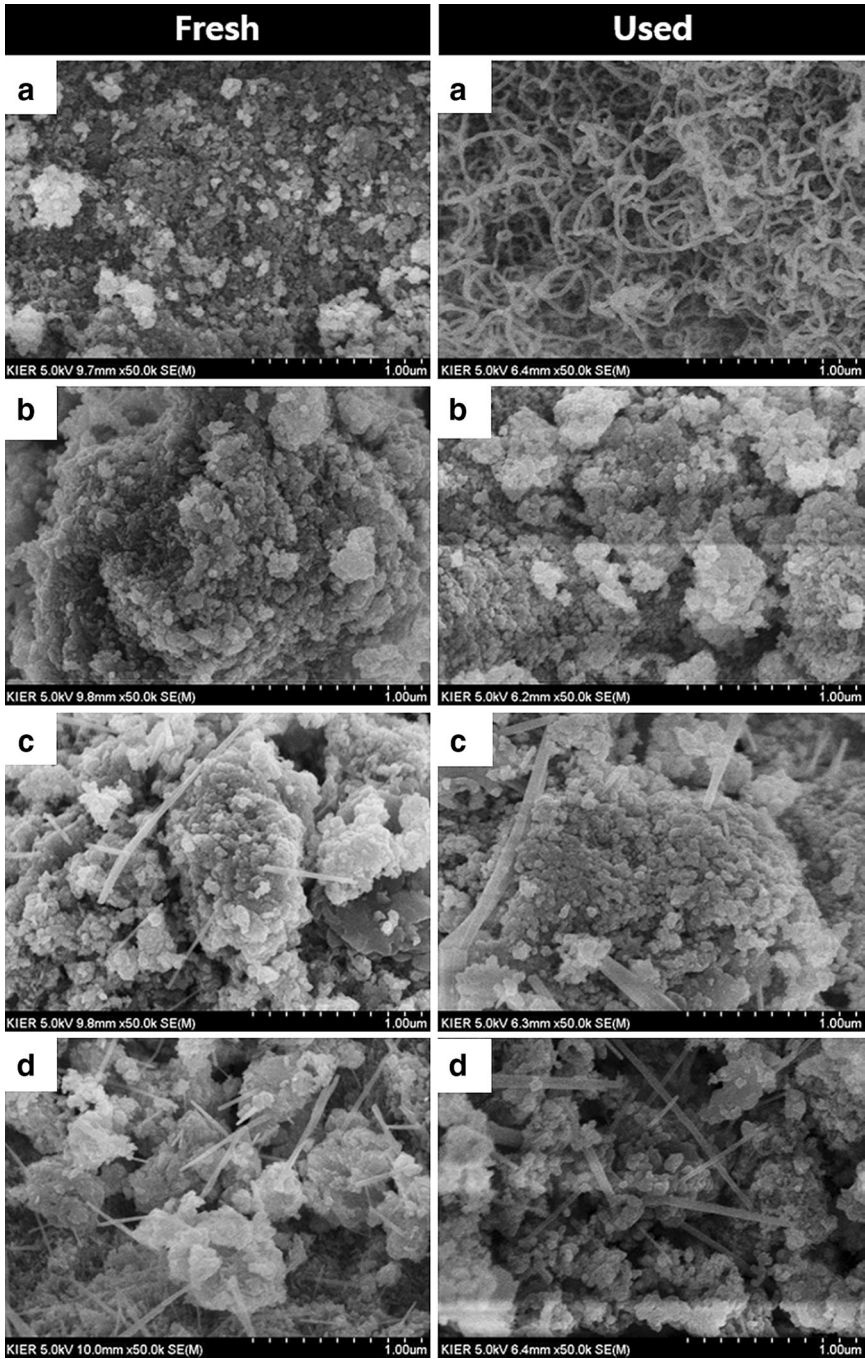


Fig. 9 SEM images of fresh and used catalysts; **a** 0K/50Ni, **b** 1K/50Ni, **c** 3K/50Ni, and **d** 5K/50Ni (reaction conditions: $T = 450\text{ }^{\circ}\text{C}$, $\text{GHSV} = 3000\text{ h}^{-1}$, $\text{S/C} = 4.0$, $\text{TOS} = 40\text{ h}$)

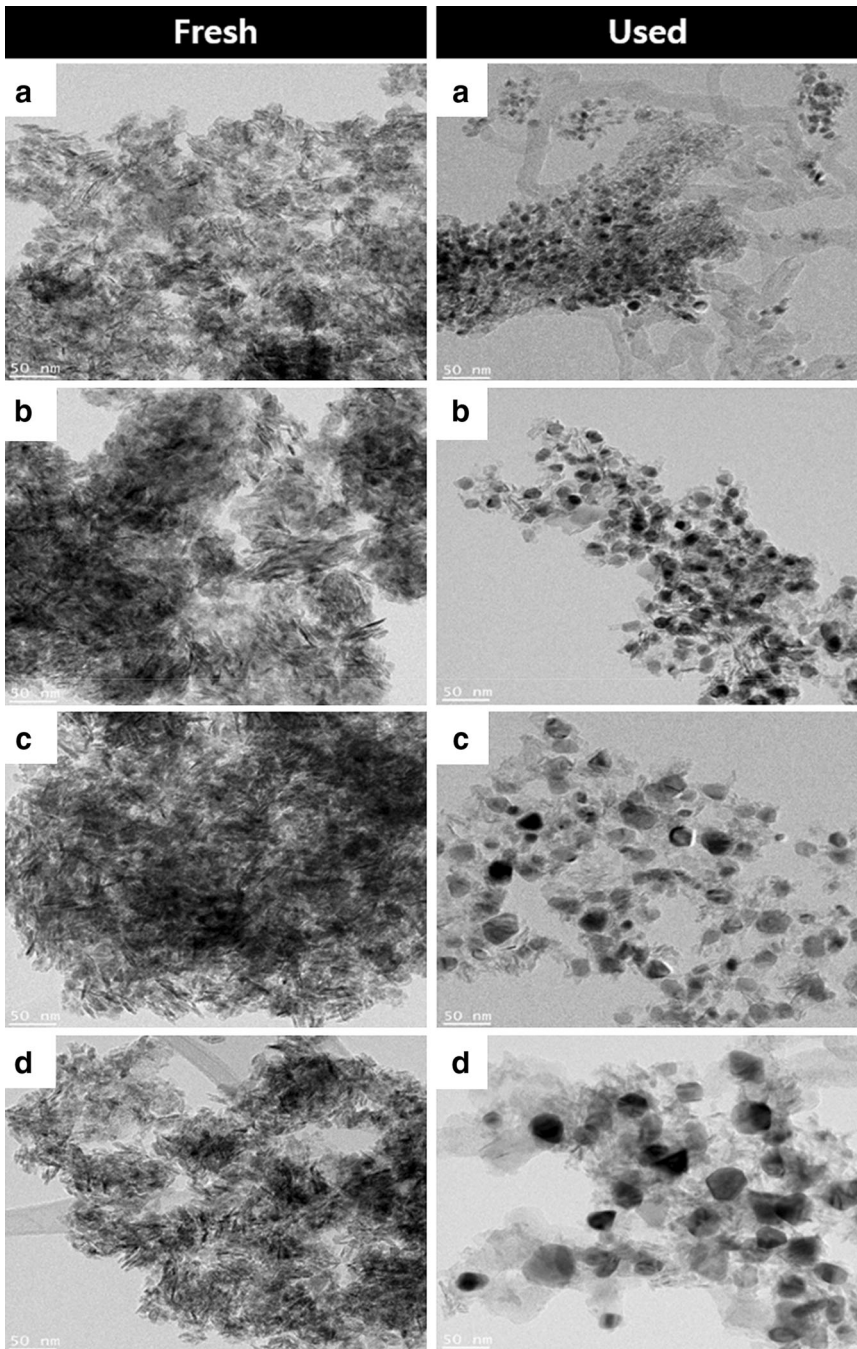


Fig. 10 TEM images of fresh and used catalysts; **a** 0K/50Ni, **b** 1K/50Ni, **c** 3K/50Ni, and **d** 5K/50Ni (reaction conditions: $T = 450\text{ }^{\circ}\text{C}$, $\text{GHSV} = 3000\text{ h}^{-1}$, $\text{S/C} = 4.0$, $\text{TOS} = 40\text{ h}$)

Table 3 Quantitative data of carbon deposited on used K promoted 50 wt% Ni/MgO–Al₂O₃ catalysts (reaction conditions: $T = 450$ °C, GHSV = 3000 h⁻¹, S/C = 4.0, TOS = 40 h)

Sample	Total amount of coke (gC/g _{cat})
0K/50Ni	0.0797
1K/50Ni	0.0200
3K/50Ni	0.0232
5K/50Ni	0.0373

Table 4 Ni crystallite size, pore diameter, and surface area of the K promoted 50 wt% Ni/MgO–Al₂O₃ catalysts

Sample	Ni crystallite size ^a (nm)		Surface area ^b (m ² /g)		Pore diameter ^b (nm)	
	Reduced ^c	Used ^d	Reduced ^c	Used ^d	Reduced ^c	Used ^d
0K/50Ni	4.9	5.5	159	154	16.1	16.1
1K/50Ni	6.0	7.9	147	134	16.1	18.5
3K/50Ni	8.4	9.5	132	104	16.1	21.3
5K/50Ni	12.2	12.3	54	82	21.3	32.3

^a The values were calculated by Scherrer's equation $2\theta = 51.6^\circ$

^b Estimated from N₂ adsorption at -196 °C

^c Reduction conditions (Heating rate = 10 °C/min, $T = 600$ °C, 4 h)

^d Reaction conditions ($T = 450$ °C, GHSV = 3000 h⁻¹, S/C = 4.0, TOS = 40 h)

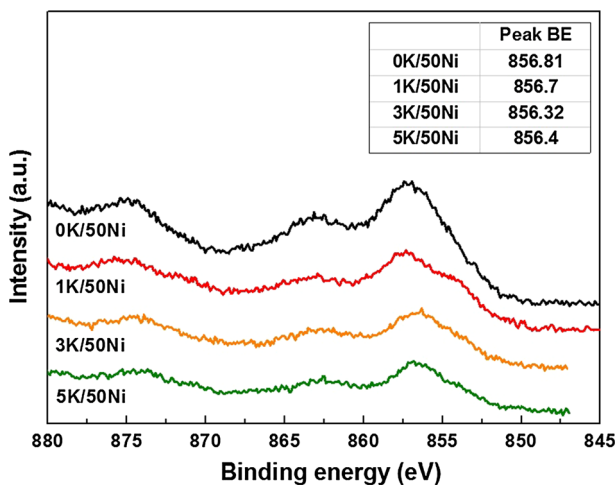


Fig. 11 XPS spectra of used catalysts; *a* 0K/50Ni, *b* 1K/50Ni, *c* 3K/50Ni, and *d* 5K/50Ni (reaction conditions: $T = 450$ °C, GHSV = 3000 h⁻¹, S/C = 4.0, TOS = 40 h)

Ni 2p_{3/2} shifts to the lower value. It is a good agreement with Juan–Juan's report that slight displacement to the lower binding energy was observed after adding potassium on the Ni/Al₂O₃ [33].

Conclusions

K addition effect on the 50 wt% /Ni/MgO–Al₂O₃ catalyst for the pre-reforming of *n*-tetradecane and its optimal content were deducted. 1K/50Ni catalyst showed stable catalytic activity at $T = 400, 450$ °C, $S/C = 4.0$, and $GHSV = 3000$ h⁻¹ conditions. However, as the amount of K loading increases, catalytic activity of the 50 wt% /Ni/MgO–Al₂O₃ catalysts were decreased. It resulted from a decrease of the Ni surface area by agglomeration of Ni particles. Coke deposition on the used catalyst was observed by SEM, TEM, and TG analysis. Deposited coke amounts of the K promoted catalysts varied from 0.0200 gC/g_{cat} to 0.0373 gC/g_{cat}. However, in the case of 0K/50Ni catalyst, 0.0797 gC/g_{cat} was deposited on the used catalyst. Among them, the 1K/50Ni catalyst showed the lowest coke deposition and stable catalytic activity during the test, and it was related to improvement of the coke resistance by K promotion.

Acknowledgments This work was supported by the New and Renewable Energy Core Technology Program of the Korea Institute of Energy Technology Evaluation and Planning (KETEP), a granted financial resource from the Ministry of Trade, Industry and Energy, Republic of Korea (201230 10040010).

References

1. J. Boon, E. van Dijk, S. de Munck, R. van den Brink, J. Power Sources **196**, 5928 (2011)
2. K. Liu, C.S. Song, V. Subramani, *Hydrogen and Syngas Production and Purification Technologies* (Wiley, NY, 2010), pp. 46–105
3. J. Zheng, J.J. Strohm, C.S. Song, Fuel Process. Technol. **89**, 440 (2008)
4. K. Shen, X. Wang, X. Zou, X. Wang, X. Lu, W. Ding, Int. J. Hydrogen Energy **36**, 4908 (2011)
5. J. Boon, E. van Dijk, *Adiabatic Diesel Pre-reforming*. Literature Survey. (Energy Research Center of The Netherlands, Petten (NL), 2008). Report no. ECN-E-08-046
6. T.S. Christensen, Appl. Catal. A Gen. **138**, 285 (1996)
7. B. Munch, P. Elholm, M. Stenseng, in *From Science to Proven Technology Development of new Topsøe Prerforming Catalyst AR-401*. Proceedings of Nitrogen + Syngas 2007 conference, Bahrain, 2007
8. F. Arena, G. Trunfio, E. Alongi, D. Branca, A. Parmaliana, Appl. Catal. A Gen. **266**, 155 (2004)
9. T. Sperle, D. Chen, R. Lødeng, A. Holmen, Appl. Catal. A Gen. **282**, 195 (2005)
10. K.Y. Koo, S.H. Lee, U.H. Jung, H.S. Roh, W.L. Yoon, Fuel Process. Technol. **119**, 151 (2014)
11. T. Osaki, T. Mori, J. Catal. **204**, 89 (2001)
12. D.L. Trimm, Catal. Today **37**, 233 (1997)
13. D.L. Trimm, Catal. Today **49**, 3 (1999)
14. X. Hu, G. Lu, Green Chem. **11**, 724 (2009)
15. F. Frusteri, F. Arena, G. Calogero, T. Torre, A. Parmaliana, Catal. Commun. **2**, 49 (2001)
16. J.R. Rostrup-Nielsen, J. Catal. **33**, 184 (1974)
17. C.E. Daza, A. Kiennemann, S. Moreno, R. Molina, Appl. Catal. A Gen. **364**, 65 (2009)
18. M.A. Ebiad, D.R. Abd El-Hafiz, R.A. Elsalamony, L.S. Mohamed, RSC Adv. **2**, 8145 (2012)
19. S.H. Park, K. Chun, W.L. Yoon, S.H. Kim, Res. Chem. Intermed. **34**, 781 (2008)
20. J.L. Colby, P.J. Dauenhauer, L.D. Schmidt, Green Chem. **10**, 773 (2008)
21. J. Kapicka, N.I. Jaeger, G. Schulz-Ekloff, Appl. Catal. A Gen. **84**, 47 (1992)
22. M.A. Ali, T. Kimura, Y. Suzuki, M.A. Al-Saleh, H. Hamid, T. Inui, Appl. Catal. A Gen. **227**, 63 (2002)
23. F. Frusteri, S. Freni, V. Chiodo, L. Spadaro, O. Di Blasi, G. Bonura, S. Cavallaro, Appl. Catal. A Gen. **270**, 1 (2004)
24. Z. Hou, O. Yokota, T. Tanaka, T. Yashima, Appl. Catal. A Gen. **253**, 381 (2003)

25. J. Juan-Juan, M.C. Román-Martínez, M.J. Illán-Gómez, *Appl. Catal. A Gen.* **301**, 9 (2006)
26. K.Y. Koo, M.G. Park, U.H. Jung, S.H. Kim, W.L. Yoon, *Int. J. Hydrogen Energy* **39**, 10941 (2014)
27. G. Trunfio, F. Arena, *Catalysts* **4**, 196 (2014)
28. C11-PR Adiabatic Pre-reforming Catalyst Product Bulletin, SÜD-CHEMIE
29. K.M. Dooley, J.R.H. Ross, *Appl. Catal. A Gen.* **90**, 159 (1992)
30. N. Iwasa, T. Yamane, M. Arai, *Int. J. Hydrogen Energy* **36**, 5904 (2011)
31. D. Varisli, N.G. Kaykac, *Appl. Catal. B Environ.* **127**, 389 (2012)
32. Y.S. Jung, W.L. Yoon, Y.S. Seo, Y.W. Rhee, *Catal. Commun.* **26**, 103 (2012)
33. J. Juan-Juan, M.C. Román-Martínez, M.J. Illán-Gómez, *Appl. Catal. A Gen.* **264**, 169 (2004)
34. T. Horiuchi, K. Sakuma, T. Fukui, Y. Kubo, T. Osaki, T. Mori, *Appl. Catal. A Gen.* **144**, 111 (1996)
35. K.Y. Koo, H.S. Roh, Y.T. Seo, D.J. Seo, W.L. Yoon, S.B. Park, *Int. J. Hydrogen Energy* **33**, 2036 (2008)